RAINFALL–RUNOFF ESTIMATION USING DIGITAL RADAR *

Russell A. Kutzman and *Peter S. Ray*

Department of Meteorology, Florida State University, Tallahassee, Florida 32306, USA

Received November 5, 1994

ABSTRACT

Storm runoff is a concern to meteorologists and hydrological forecasters. A radar basin–based runoff algorithm is presented. The algorithm is based on the relationship between the rainfall over the basin and the discharge response at the gauge station. The algorithm is designed to provide runoff as a function of time for a given input(s) of rainfall. With known overflow levels, flood potential can also be evaluated. The runoff algorithm examined outflow at five basins within the operating scope of the Pittsburgh National Weather Service (NWS) radar. A comparison of the observed runoff was made with the algorithm generated discharge. In general, hydrograph accuracies improved with increasing rainfall excess. Possible reasons for discrepancies are examined.

Key words: rainfall, runoff, digital radar, hydrograph

I. INTRODUCTION

Devastation and loss of life document the nature of floods. The impact is often magnified due to population centers being situated near water. As a result, the need for hydrological forecasting and flood control systems are necessary to minimize the effects of these natural disasters.

Over the past three decades, flood prediction studies centered around the modeling of runoff in watersheds. The advent of computer technology enabled researchers to approach this problem using several methods. Hydrological systems can be deterministic or stochastic, linear or nonlinear, time invariant or time dependent, lumped or distributed (Delleur and Rao 1973).

The runoff algorithm inputs actual or forecasted reflectivities or precipitation accumulations and computes storm runoff as a function of time for each basin. With predetermined river threshold values, the algorithm also evaluates flood potential and the time the river's capacity will be exceeded. A forecast will be made at each basin within the operating range of the radar site. The runoff algorithm is just one of a series of Tropical Weather Hazard algorithms, each designed to estimate specific aspects of threatening hurricanes and typhoons.

The factors influencing the runoff process include (1) precipitation, (2) interception, (3) infiltration, (4) evaporation, (5) transpiration, (6) groundwater flow, (7) surface runoff and (8) channel flow. In some form, they all must be considered. A partial list of references follows. Precipitation has been treated by Wilson (1990); interception by Linsley et al. (1949), Dunne and Leopold (1978), Patric (1965) and Leyton et al. (1967); infiltration by Horton (1933) and Foster

* Computer support was provided by Bret Whissel. Partial support for this research was from the Paramax Corporation Grant number 1338—64542.

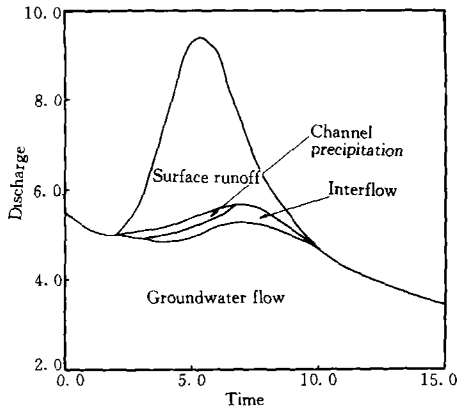

Fig. 1. Components of the hydrograph.

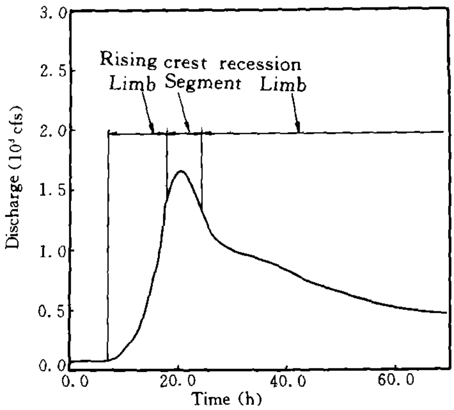

Fig. 2. Regions of the hydrograph.

(1948); depression storage by Linsley et al. (1949); evaporation by Wilson (1990); transpiration by Dunne and Leopold (1978), Thornthwaite (1948) and Penman (1948); and groundwater flow by Wilson (1990), Viessman et al. (1977) and Dunne and Leopold (1978); runoff by Horton (1934), (1945); and channel flow by Dunne and Leopold (1978), Chezy (1769), Manning (1889).

Although it is possible to derive the runoff from the physics of each of these components of the hydrological cycle, their effect is integrated in the hydrograph, or the continuous record of the discharge versus time. In most hydrograph analyses, interflow and channel precipitation are lumped together with surface runoff. Channel precipitation is the fastest and immediately adds to the outflow. Its contribution is usually only a small fraction of total flow. As pointed out by Linsley et al. (1949), the water surface area for most basins does not exceed five percent of the total area at fairly high stages. Interflow is part of the subsurface flow which moves at shallow depths and reaches the surface channels in fairly short time periods. Its distribution is commonly characterized by a slowly increasing rate up to the end of the storm period, followed by a gradual recession which terminates at the intersection of the surface flow hydrograph and the base flow hydrograph (Viessman et al. 1977). Figure 1 shows the various contributions of each component.

The shape of the hydrograph for a single, short–duration storm has three distinct characteristics: a rising limb, a crest segment, and a recession limb. Figure 2 shows these hydrograph components for a uniform rainfall event. The inflection points separate the crest segment from the rising and falling limbs. The falling part of the hydrograph can be thought of as a combination of recession curves. The storage accumulations from surface runoff, baseflow and interflow will slowly deplete once rainfall ends. For small catchment areas, total contributions by groundwater flow, channel precipitation, and interflow are relatively small in comparison to the amount received by surface runoff.

Timing parameters are essential to understanding the relationship between rainfall and runoff. Figure 3 explores the terminology associated with a typical storm hydrograph and a rainfall hyetograph. The following timing aspects are defined:

1) Lag to peak (L): time from the center of mass of rainfall excess to peak of the hydrograph;

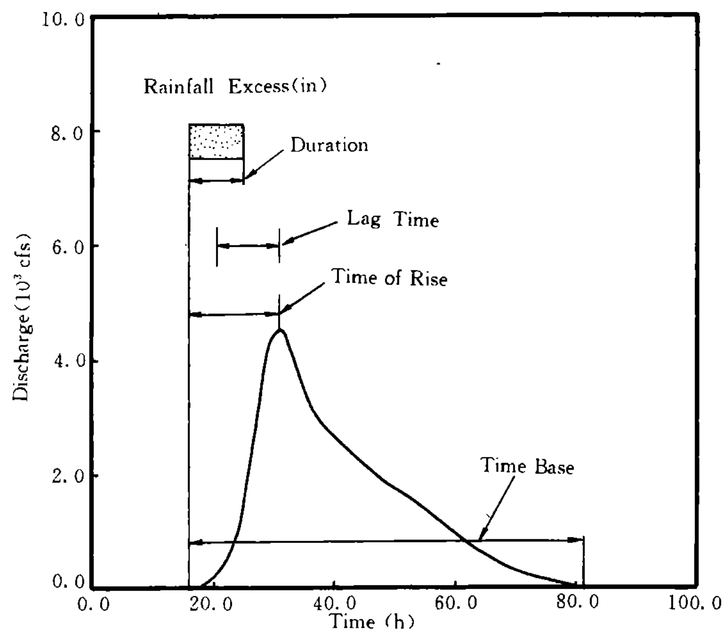

Fig. 3. Terminology associated with the runoff hydrograph.

2) Duration (D): length of time during which rain falls;

3) Time base or base length (T_b): length of time of surface runoff;

4) Time–of–rise (T_R): time from the start of rainfall excess to the peak.

1. *Factors Affecting Hydrograph Sharp*

The time distribution of runoff is determined by the physical characteristics of the basin, and the climatic factors. The rising limb and the peak are functions of history and rainfall intensity as well as of basin characteristics, while the recession limb is largely independent of the storm details producing runoff (Ward 1967).

(1) *Climatic factors affecting hydrograph shape*

The climatic factors which influence hydrograph shape and the runoff volume are (1) rainfall intensity and duration; (2) rainfall distribution over the basin; (3) direction of storm movement; and (4) type of precipitation and type of storm.

(2) *Physical factors affecting hydrograph shape*

The primary physical characteristics of drainage basins are its area, shape, elevation, slope, soil type, timing distribution, and peak discharge of runoff. The surface–runoff hydrograph represents the integrated effect of all the basin's physical characteristics and their modifying influence on the translation and storage of rainfall excess. The factors involved are numerous, some having a major bearing on the phenomena and others being of negligible consequence. It is difficult to cover the influence of each individual factor in detail. The effect of each factor may be obscured by the effect of another (Gray 1973). The following list describes the basin's physical characteristics that hydrologists consider to have the main influence on hydrograph shape.

2. *Unit Hydrograph*

The determination of runoff from precipitation measurements had its origins with hydrograph analyses. In 1932, Sherman conceived the idea of the unit hydrograph, as "basin outflow resulting from one inch (one centimeter) of direct runoff generated uniformly over the drainage area at a uniform rainfall rate during a specified period of time". The unit hydrograph concept has several assumptions limiting its usefulness in all rainfall–runoff scenarios:

1) For a given watershed, rainfall excesses of equal duration are assumed to produce surface runoff hydrographs with equivalent time bases regardless of the intensity of the rain.

2) For a given watershed, the magnitude of the runoff ordinates for a storm of a given duration is assumed directly proportional to rainfall excess volumes. Thus, twice the rainfall produces a doubling of the hydrograph ordinates.

3) For a given watershed, the time distribution of direct runoff from a given storm is assumed independent from antecedent or subsequent storm periods.

The unit hydrograph theory is predicated on the system being linear and time–invariant. However, these assumptions are incorrect. The relationship between rainfall excess and surface runoff in a basin is nonlinear. Laboratory testing supports channel flow theory such that greater depths of water move faster and would therefore alter runoff reponse. Furthermore, antecedent conditions change the infiltration rate and depression storage resulting in a reduction of total rainfall. However, for most runoff models the linearity guidelines produce results consistent with those using nonlinear criteria.

The requirements to analyze runoff involve only two inputs: excess rainfall and the unit hydrograph. The simplicity in the input / output relationship enables runoff modeling with a minimum of calculations. The complexities of the hydrological cycle and each basin's physical characteristics are assumed fixed and inherently incorporated within the unit hydrograph. Therefore, the response of a linear basin to any rainfall excess input is directly proportional to the unit hydrograph. All aspects of the models physics and hydrology are replaced by the linear response function. The unit hydrograph construction will be explored in the methodology section.

Most practical techniques of forecasting runoff from rainfall are based on either correlation techniques between observed volumes of rainfall and runoff or on the unit hydrograph method. The hydrograph method is a "black box" technique. It is therefore not a tool which will aid in the understanding and development of the physics involved (Raudkivi 1979).

The unit hydrograph is most easily derived from the hydrograph of a single isolated rainfall. To be able to use the unit hydrograph to determine the runoff from different storms, the selection of the proper storm duration is important. Opinions vary widely depending on whether the basin is large or small. Linsley et al. (1949) cite that in practical applications, experience has shown that the time unit employed should approximate one–fourth of the basin lag time. They suggested that the effect of small differences in storm duration is not large and that a tolerance of ± 25 percent from the adopted unit hydrograph duration is accepted.

The United States Army Corps of Engineers (1948) found that values of unit–storm duration equal to about half of the basin lag time appear to be satisfactory. This criteron is used for basins of less than 100 square miles.

Once the hydrograph has been determined, estimating the runoff from rainfall excess can begin. From the unit hydrograph for any duration of uniform rain, the unit hydrograph for any other duration can be obtained. As the duration becomes shorter, the resulting unit hydrograph approaches an instantaneous hydrograph. The instantaneous hydrograph (IUH) is the hydrograph of runoff that will result if an inch of water is spread uniformly over an area and then allowed to runoff (Schaake 1965).

From a mathematical perspective, the ordinates of the IUH represent the relative effect of antecedent rainfall intensities on the runoff rate at any instant of time. By plotting the IUH with time increasing to the left rather than to the right and then superimposing this plot over the excess rainfall hydrograph (plotted with time increasing to the right), the relative weight given to antecedent rainfall intensities is easily seen. The runoff rate at any time is computed as a weighted average of the previous rainfall intensities. The computed runoff hydrograph is the weighted, moving average of the excess rainfall pattern and the weighting function is the time–reversed image of the unit hydrograph (Schaake 1965).

The surface runoff rate can be expressed mathematically as

$$Q(t) = \int_0^t f(\tau) i(t-\tau) \mathrm{d}\tau, \tag{1}$$

where $Q(t)$ is the surface runoff at time t, $f(\tau)$ the ordinate of the IUH at time τ, and $i(t-\tau)$ the excess rainfall intensity at time $t-\tau$.

The variable τ represents time into the past so that time $t-\tau$ occurs before time t. The limits of the integral allow τ to vary from the present time back through a duration equal to the hydrograph's baselength. The integral gives a continuous weighting of previous rainfall intensities by the ordinates of the IUH.

3. *Measuring Storm Rainfall by Radar*

The use of radar is a very common technique to evaluate rainfall accumulation as well as rainfall patterns. Radar scans are presentations of instantaneous back–scattered microwave energy. These depictions correspond to the number and sizes of water or ice scatted within the viewing field. When precipitation particles are small with respect to the radar wavelength, the back–scattered power can be related to a rainfall rate.

II. METHODOLOGY

Flows in five drainage basins along the Alleghany River were chosen to verify runoff from several precipitation events. Using digitized radar reflectivity data from the NWS radar at Pittsburgh and unit hydrograph techniques, storm runoff and its timing characteristics are determined at each gauge station.

The runoff algorithm is a three–step procedure: basin mapping and accumulation processing, unit hydrograph determination, and runoff / flood potential execution. The basin mapping and the unit hydrograph development are preparatory steps that must be accomplished only once for each basin.

1. *Basin Description*

The five drainage basins are situated in the southwest corner of Pennsylvania. Figure 4 shows the spatial relationship between the basins and the radar site. To illustrate the

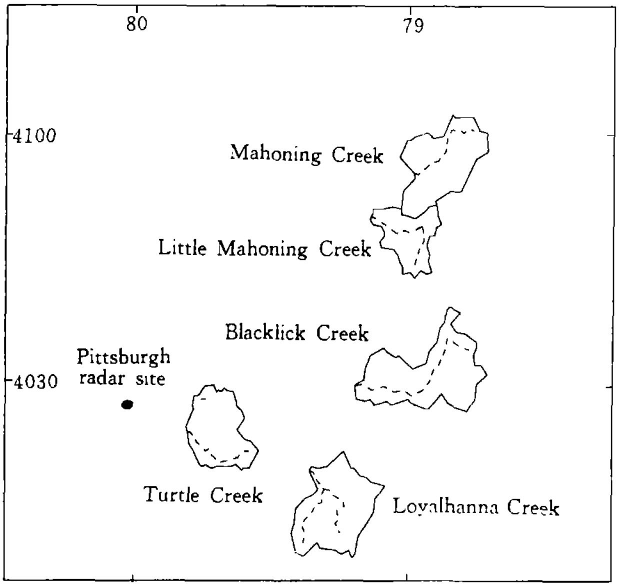

Fig. 4. Illustration of the five drainage basin locations relative to the Pittsburgh radar site. The dashed line shows the orientation of the main stream trunk.

geomorphical diversity between basins and ultimately the universal application of unit hydrograph techniques, Table 1 lists each of the basin's main physical characteristics. These variables, to varying degrees, form the basis for the runoff response function. Each basin has a unique curve, mirroring the basin and channel network properties. The following definitions help clarify the nomenclature used in the table:

Table 1. Drainage Basin Characteristics from Wetzel and Bettandorff (1986)

Creek	Blacklick	Loyalhanna	Turtle	Mahoning	Lil Mahoning
Area (mi^2)	192.0	172.0	55.9	158.0	87.4
Slope (ft / mi)	21.0	23.0	21.0	9.51	16.8
Length (mi)	40.6	21.1	15.1	26.9	24.16
Elevation (ft)	1780	1730	1120	1570	1550
Forest cover (%)	47.0	71.0	47.0	69.0	44.0
Annual precipitation (in)	46.0	47.2	41.0	43.2	44.3
Storage (%)	0.10	1.3	1.0	1.1	1.0

Note: 1 mi≈1.609 km; 1 in≈2.54 cm.

1) Drainage area (AREA) is the area that contributes directly to surface runoff.

2) Main channel slope (SLOPE) is the difference in elevation at points 10 and 85 percent of the distance along the channel from the gauging station to the basin's rim, divided by the distance between the two points.

3) Main channel length (LENGTH) is the length the channel from the gauging station to

the basin divide.

4) Mean base elevation (ELEVATION) is the average height, in feet, above National Geodetic Vertical Datum of 1929.

5) Forest cover (FOREST COVER) is the ratio of the forest cover, as shown on Geological Survey maps, to the drainage area.

6) Storage (STORAGE) is the percentage of the drainage area that includes lakes, ponds, and wetlands as shown on topographic maps.

2. *Radar Data Processing*

Pittsburg NWS Radar Data Processor (RADAP II) archived data provide the reflectivity information necessary to determine rainfall accumulations over each basin. Based on the strength of the signal returned from the target, the radar receiver would estimate an equivalent reflectivity factor (in $mm^6\ m^{-3}$). The reflectivity factor (Z) ranges from approximately 50 to 500 000 $mm^6\ m^{-3}$. The receiver then calculates the logarithm of each estimated value of Z; the dynamic range of $\log Z$ is about 1.7 to 5.9. To further simplify data processing, the $\log Z$ is scaled upwards by a factor of 10 ($10 \log Z$); these values are commonly referred to as dBZ values.

The RADAP II computer takes base elevation (0.5 degrees) observations every ten minutes. Each observation consists of 180 radials at ranges from 10 to 125 nautical miles. The data are divided into 20 700 grid boxes, each grid box is 1 nautical mile by 2 degrees of azimuth. Estimated radar rainfall rates are computed using the Z–R relationship:

$$Z = 200R^{1.6}, \tag{2}$$

developed by Marshall and Palmer (1948). The data values range from 0 to 15 with each nonzero value representing a RADAP II category of radar reflectivity.

3. *Hydrograph Determination*

Viessman et al. (1977) cite that in developing a unit hydrograph, it is desirable to get as many rainfall records as possible within the study area to insure that the amount and distribution of rainfall over the watershed is accurately known. Preliminary selection of storms to use in deriving a unit hydrograph should be restricted to:

1) Storms occurring individually, that is simple storm structure.

2) Storms having uniform distribution of rainfall throughout the period of excess rainfall.

3) Storms having uniform spatial distribution over the entire watershed.

Several other restrictions are used as guidelines. The sizes of the basin should not exceed 1000 mi^2. One thousand acres is typically used as the lower limit; however, numerous physical factors define an appropriate response function. Studies indicate that direct runoff should range from 0.5 to 2.0 in. Finally, the duration of rainfall excess, D, should be approximately 20 to 30 percent of the basin lag time.

To determine the unit hydrograph for a drainage basin, it is necessary to separate outflow at the gauge site two components: baseflow and surface runoff. During large storms, the maximum rate of discharge is just slightly affected by baseflow, inaccuracies in separation are fortunately not important (Bedient and Huber 1988). Several separation techniques have been devised but none is based on hydrological principles. Most hydrologists agree that whatever method is used, it must be employed consistently throughout the analysis.

The method used in this experiment required plotting the hydrograph. The separation is accomplished by joining a straight line from the beginning of surface runoff to a point on the recession limb representing the end of direct runoff.

Usually, little difficulty is encountered in determining the start of the surface runoff; however, the break between the baseflow recession and direct runoff may be difficult to pinpoint. The recession limb of the hydrograph represents a series of depletion curves for the various components—baseflow, interflow channel precipitation, and surface flow. It can be described mathematically as

$$Q_2 = Q_1 K^{-\triangle t}, \qquad (3)$$

where Q_2 is the instantaneous discharge at time, t_2; Q_1 the instantaneous discharge at time, t_1; K the recession constant; and $\triangle t = (t_2 - t_1)$, the elapsed time.

This equation produces a straight line when plotted on semi–logarithmic paper. Because of the effects of the different components of storage, the plot will be curvilinear having a series of line segments of different slopes (Gray 1973). Each line segment's slope reflects the rate of decrease of discharge to the draining off process. The end of the direct runoff occurs at the beginning of the last curvilinear segment——the intersection of the baseflow recession curve with the total recession curve.

After separating the direct surface runoff from the baseflow, plot the direct runoff ordinates. The area under the curve represents the total volume of runoff. Area computations can be accomplished by planimeter, computer graphical techniques, or by using squared paper. The rainfall excess from the storm is calculated by dividing the total volume of direct runoff by the basin's area. This value can also be thought of as the equivalent depth of runoff spread uniformly over the basin (Shaw 1988).

The rainfall excess describes that portion of total rainfall that becomes direct runoff. Using the rainfall hyetograph, convert total rainfall to effective rainfall by applying the φ index infiltration method. The φ infiltration method assumes that the total volume of storm period loss is distributed uniformly across the storm pattern. The volume of precipitation above the index line is equivalent to the runoff (rainfall excess). After calculating the part of the total rainfall that constitutes rainfall excess, determine the duration (D) of the rainfall excess.

Divide the time axis of the hydrograph into convenient intervals. The interval duration most frequently used is hourly or some multiple of the radar scan period. The corresponding runoff ordinates to the time intervals are divided by the rainfall excess in inches (cm). Plot these results as a unit hydrograph for the basin.

Check the volume of the unit hydrograph. The area under the curve is equivalent to 1.0 inch over the entire basin's area. Graphically adjust the ordinates as necessary.

Repeat the procedure for a number of storms that meet the criteria. Obtain an average hydrograph for the basin (see Fig. 5). The average hydrograph may be constructed by taking the arithmetic mean of the peak flows and the times–of–rise. Using the previous two values as reference points, draw the hydrograph to match the general shape of the individual unit hydrographs.

Once the mapping and unit hydrograph procedures are completed, the actual execution of the runoff algorithm can begin.

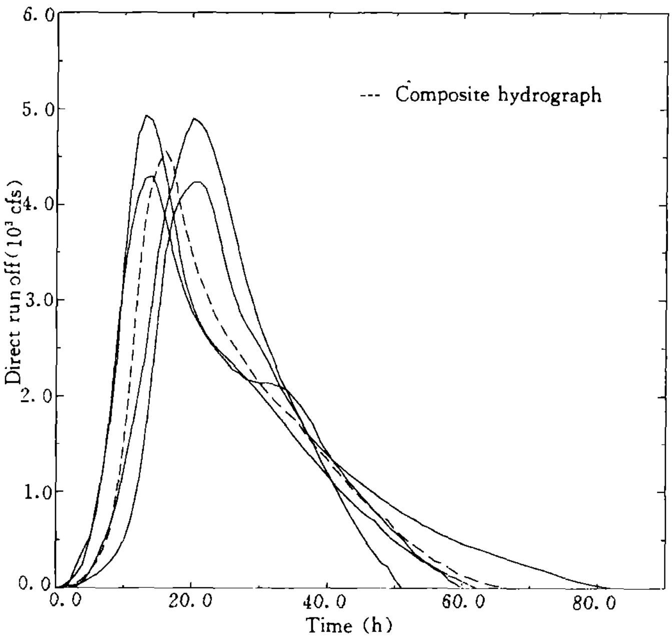

Fig. 5. Derivation of a unit hydrograph from storms.

The first step in this procedure is to process the reflectivity data. Each scan is read by the computer, the reflectivity values are added together. Next, the reflectivity sum is divided by the total number of bins within each basin to get an average reflectivity value. The average basin reflectivity value is converted to an hourly rainfall accumulation using a reflectivity / rainfall relationships.

Six hourly scans are processed to give one hourly rainfall estimate. Hourly estimates are used in this experiment because the available outflow data are measured on an hourly basis. Measurement intervals should be adapted to meet optimum experiment goals. Small basins (< 10 mi^2) have faster response functions and therefore may need shorter evaluation intervals.

After the rainfall accumulations are evaluated, these values are reduced by a constant infiltration rate. The resultant measurements reflect a rainfall excess for each time interval. Infiltration rates may be taken from basin geological survey reports or from averaging the portion of the hydrographs after the rainfall excess has been removed. This value, a measure of the infiltration rate, reflects the difference between the total rainfall and the rainfall excess.

The linear response of a basin to any rainfall input is proportional to the unit hydrograph. This proportionality can be generalized to compound storms as well as individual events.

4. *Flood Prediction*

After summing the products of rainfall excess and basin response inputs, the stream flow hydrograph is plotted and flooding potential can be examined. To simplify the problem, hydrologists typically investigate the relationship between river height and discharge. River height or stage refers to the elevation of the water surface above some arbitrary datum (Dunne and Leopold 1978). A rating curve can be developed if discharge is simultaneously plotted against the corresponding stage. Once this relationship is established, the river's threshold value is determined. Flood potential can be computed as

$$FLD - POTENTIAL = \left[\frac{RUNOFF + BASEFLOW}{THRESHOLD} \right] \times 100, \tag{4}$$

where *FLD−POTENTIAL* equals probability of flood occurrence (%), *RUNOFF* is maximum predicted runoff ordinate (cfs)[1], *BASEFLOW* is average baseflow rate for the basin (cfs), and *THRESHOLD* the river's maximum flow capacity (cfs).

If the flood potential exceeds 100 percent, a flood near the gauging station is likely. Inferences about the flooding probability both upstream and downstream require careful examination. Basin thresholds vary and extending flood criteria to other locations should be done on a case–by–case basis.

Once the river's capacity has been surpassed, the flood time is computed. This time will be differentiated from the stream flow hydrograph. If necessary, the flood inundation period can also be assessed. The duration is measured by subtracting the time the bank overflowed from the anticipated time the level will recede below the critical flow capacity.

III. RESULTS

Runoff analysis at the five watersheds was accomplished using the Pittsburgh RADAP II data, basin unit hydrographs, and Army Corps of Engineers discharge data. After the radar reflectivity data were processed into hourly accumulations, each rainfall increment was reduced by a constant basin infiltration rate. Next, the discrete form of the convolution integral was applied. Unit hydrograph ordinates were multiplied by rainfall excess and lagged in sequence to produce the resulting storm hydrograph. All time increments of rainfall excess correspond to the duration of the unit hydrograph——one hour intervals.

Each unit hydrograph response curve reflects the basin's unique behavior to one inch of uniformly distributed rainfall excess. The curves are composites from basin outflow data from 1986—1989. A minimum of four unit hydrographs was used to establish each basin's average unit hydrograph.

Examining the unit hydrograph plot (see Fig. 6), the volume of runoff for each basin is proportional to the area under each curve. Blcaklick Creek (192 mi^2), has the greatest runoff volume (measured in million cubic feet (mcf)). Alternatively the smallest basin, Turtle Creek (55.9 mi^2), has the least runoff volume per rainfall input.

On the other hand, Turtle Creek (6247 cfs) has the highest runoff peak while Little Mahoning Creek (3953 cfs) has the lowest one. The runoff peak is the most significant hydrograph feature. The moment of greatest danger and maximum inundation occurs at this point. Turtle Creek's sharp peak reflects the explosive nature of its runoff response. Flood potential is greatest at this time.

Even though Blacklick Creek has a larger basin area to contribute direct runoff, the discharge response function is spread over a longer time period. Subsequently the peak is less severe but if a flood should occur, duration of damage will most likely be longer. No generalized hydrological relationships should be drawn from these assessments. The comparisons are only

[1] 1 cfs = $2.831685 \times 10^{-2}\ m^3\ s^{-1}$.

highlighted for the purpose of seeing how close these patterns are maintained during the actual rainfall / runoff case studies.

The final timing parameter associated with the statistical likelihood of a flood is the time–of–rise. The duration from the runoff start to the peak discharge is critical in flood prediction. This is largely because people generally do not become concerned with flooding until actual flood conditions have been reached (Sheaffer 1961). Again Turtle Creek (7 h) shows the most rapid time response to peak runoff. Blacklick Creek displays the slowest time–of–rise (19 h).

The accuracy of the unit hydrograph technique was explored through the hydrograph characteristics in addition to a comparison of the track's shape. Usable radar reflectivity data for the Pittsburgh area were limited to March through October 1989. Because the number of precipitation days was limited, the sample size is too small to statistically generalize the technique results to all rainfall / runoff events.

The acceptability of the unit hydrograph technique was measured by how well the predicted runoff parameters compared with the measured ones. The forecast and measured runoff (total discharge–baseflow) values were both scrutinized at the gauge stations. The hydrograph characteristics were evaluated by the following two error analysis methods:

$$\varepsilon = \tilde{r} - r \tag{5}$$

and

$$\varepsilon_r = \frac{\varepsilon}{r} = \frac{\tilde{r} - r}{r}, \tag{6}$$

where ε is absolute error, $\tilde{r}$ predicted variable, r observed variable, and ε_r relative error. Eqs. (5) and (6) represent the absolute and relative errors, respectively, between the flood variables evaluated in this experiment. Hydrograph technique results were examined on a basin by basin basis.

Two types of errors are most apparent. The first is in the amplitude of the run off, and the second is in the phase of the peak, or time–of–rise. Of course, both can occur simultaneously.

1. *Blacklick Creek Hydrograph Analysis*

Five radar recorded precipitation events in 1989 were used to verify runoff characteristics for the Blacklick Creek basin. Other rainfall events during the year were unable to generate significant runoff. For this basin, a minimum average internal RADAP level greater than 2 (0.07 in / h) is needed to obtain a rainfall rate high enough to produce runoff once a constant infiltration loss was subtracted. A φ infiltration rate of 0.07 in / h was used for the Blacklick Creek watershed. The details are listed in Table 2.

The March 28 storm is the first and strongest precipitation–producing event used for Blacklick Creek. Because of the shorter runoff duration, the predicted runoff volume was 12% lower. The observed rainfall excess (total runoff volume divided by the basin area) of 0.85 inches compared favorably to the total radar determined rainfall (0.96 in) once the basin infiltration rate (0.07 in) was subtracted. As a result of the shorter time base, the predicted rainfall excess (0.74 in) was 12.9% lower than the observed value.

An examination of peak outflow revealed the predicted maximum value (4002 cfs) was 133 cfs higher than the observed peak. The peak runoff difference represented a 3.4% relative error. The times–of–rise for this event suggested a faster response time for the observed track (18 h) as compared to the predicted one (21 h). As a whole, the predicted track was in close agreement with the observed track.

Table 2. Rainfall Characteristics for Blacklick Creek

Date (1989)	28 March	31 March	18 April	28 June	30 July
Radar rainfall (in)	0.96	0.47	0.25	0.24	0.48
Duration (h)	3	1	1	2	1
Basin radar coverage (%)	64	57	96	99	99
Observed runoff volume (mcf)	378.1	179.8	149.3	56.5	270.4
Predicted runoff volume (mcf)	332.1	175.5	77.9	44.2	180.2
Absolute error (mcf)	−46.0	−4.3	−71.4	−12.3	−90.2
Relative error (%)	−12.2	−2.3	−47.8	−21.8	−33.3
Observed rainfall excess (in)	0.85	0.40	0.33	0.13	0.61
Predicted rainfall excess (in)	0.74	0.39	0.17	0.10	0.40
Absolute error (in)	−0.11	−0.01	−0.16	−0.03	−0.21
Relative error (%)	−12.9	−2.5	−48.5	−23.1	−34.4
Observed peak (cfs)	3869	2244	1519	619	3173
Predicted peak (cfs)	4002	2148	967	533	2202
Absolute error (cfs)	133	−56	−552	−86	−971
Relative error (%)	3.4	−2.5	−36.3	−13.9	−30.6
Observed time–of–rise (h)	18	19	22	34	21
Predicted time–of–rise (h)	21	19	19	20	19
Absolute error (h)	3	0	−3	−14	−2
Relative error (%)	16.7	0	−13.6	−41.1	−9.5

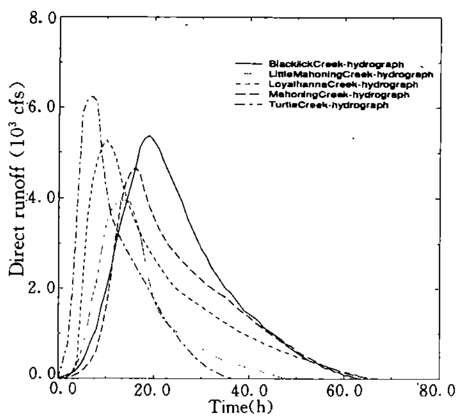

Fig. 6. A comparison of the five basin's unit hydrographs used in this experiment.

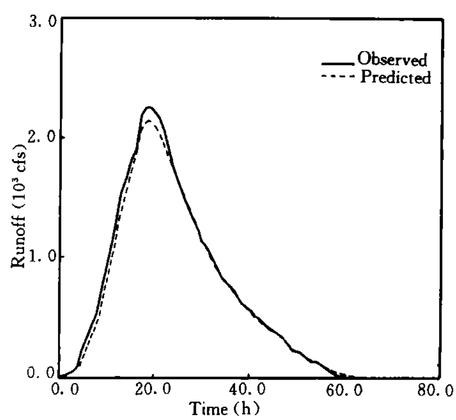

Fig. 7. Observed and predicted hydrograph tracks for Blacklick Creek, 31 March 1989.

The next precipitation case study occurred three days later on March 31. The observed and predicted tracks are nearly identical (see Fig. 7). These results are representative of the times where agreement was good. For this basin, that includes the 28 March event.

April 18 marks the third precipitation event. The hydrograph shapes were similar but the amplitude was substantially different. In addition, the observed track has a sawtooth notch prior to the peak outflow. These shape characteristics were not evident in the predicted track. Furthermore, the observed runoff was almost twice (47.3%) the predicted volume.

The observed rainfall excess was higher (by 0.08 in) than the radar determined rainfall accumulation—even without an infiltration rate reduction. Two sources of error are possible: the radar underestimates the rainfall accumulation or the discharge data were in error. Blacklick Creek had radar reflectivity returns in 96% of the bins so coverage criteria was in agreement with unit hydrograph assumptions. Additional data are needed to determine the relative importance of the error sources.

Likewise, the observed peak outflow (1519 cfs) differed considerably from the predicted outflow (967 cfs). Also the time–of–rise for the observed track (22 h) occurred three hours later than the predicted track (19 h). The critical failure of the predicted track was its underestimation of possible flood conditions. Even though the outflow was low, the error between hydrograph variables was considerable.

The fourth case study occurred on June 28. The predicted peak occurred earlier than that observed. Runoff volumes were comparatively low. The two hour radar rainfall accumulation of 0.24 inches did not follow the trend of the several rises and falls in the observed runoff. This could be the result of hourly rainfall averaging reducing usable radar rainfall reflectivities below the runoff criteria. In addition, smaller rainfall variations were smoothed in the convolution process. This phase error is illustrated in Fig. 8.

July 30 were the final data for the Blacklick Creek case study. The hydrograph shapes are consistent although the predicted track underestimates the magnitude of the runoff. The relative error between the two runoff volumes is −33%. Again as in the April 18 case study, the observed

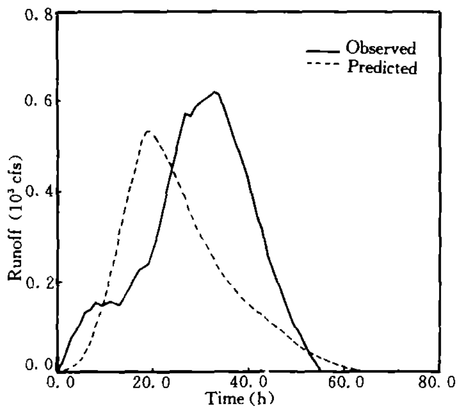

Fig. 8. Observed and predicted hydrograph tracks for Blacklick Creek, 28 June 1989.

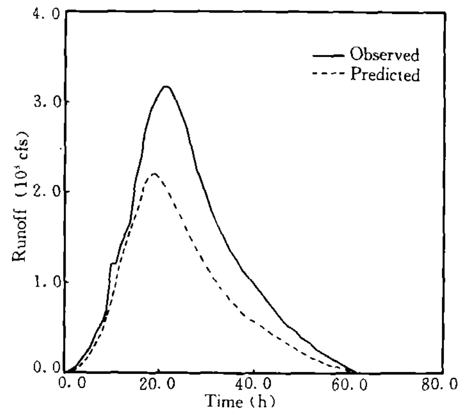

Fig. 9. Observed and predicted hydrograph tracks for Blacklick Creek, 30 July 1989.

rainfall excess exceeds the total radar determined value. In this instance the difference is 0.13 inches. The radar determined accumulation (0.48 in) falls close to the recommended depths for hydrograph analysis. However, observed rainfall excess should not exceed radar derived values. Examination of further Blacklick Creek events should concentrate on the possibility of a systematic radar rainfall underestimate. A secondary rain gauge network would be helpful in verifying measurements. This comparison is illustrated in Fig. 9, and illustrates a case where there is amplitude error, such as for 18 April case.

2. *Little Mahoning Creek Hydrograph Analysis*

Little Mahoning was the next watershed to be examined. This basin case study contains seven precipitation events. The results are tabulated in Table 3.

Table 3. Rainfall Characteristics for Little Mahoning Creek

Date 1989	18 Mar.	28 Mar.	30 Mar.	31 Mar.	15 May	27 June	19 Oct.
Radar rainfall (in)	0.23	0.90	0.53	0.47	0.19	0.32	0.11
Duration (h)	2	2	2	1	1	1	1
Basin radar coverage (%)	63	66	61	86	99	69	100
Observed runoff volume (mcf)	35.2	194.7	79.2	93.4	55.7	87.8	43.3
Predicted runoff volume (mcf)	28.5	173.8	94.0	91.1	30.5	59.1	13.1
Absolute error (mcf)	−6.7	−20.9	14.8	−2.3	−25.2	−28.7	−30.2
Relative error (%)	−19.0	−10.7	18.7	−2.5	−45.2	−32.7	−69.7
Observed rainfall excess (in)	0.17	0.96	0.39	0.46	0.27	0.43	0.21
Predicted rainfall excess (in)	0.14	0.85	0.46	0.45	0.15	0.29	0.06
Absolute error (in)	−0.03	−0.11	0.07	−0.01	−0.12	−0.14	−0.15
Relative error (%)	−17.6	−11.4	17.9	−2.0	−44.4	−32.6	71.4
Observed peak (cfs)	517	3284	1658	1792	857	1272	401
Predicted peak (cfs)	512	3159	1693	1660	553	1067	237
Absolute error (cfs)	−5	−125	35	−132	−302	−205	−164
Relative error (%)	−1.0	−3.8	2.1	−7.4	−35.5	−16.1	−40.9
Observed time−of−rise (h)	16	14	14	15	17	13	19
Predicted time−of−rise (h)	14	14	14	14	14	14	14
Absolute error (h)	−2	0	0	−1	−3	1	−5
Relative error (%)	−12.5	0	0	−6.7	−17.6	7.7	−26.3

An examination of the March 18 hydrographs reveals nearly identical predicted and observed hydrographs. Radar bin coverage was 63%. The infiltration rate (0.05 in / h) reduced radar accumulation (0.18 in) agrees with the observed (0.17 in) and predicted (0.14 in) rainfall excesses. However, the observed and predicted runoff volumes differed by 19%. The peak runoff totals almost match for the observed (517 cfs) and predicted (512 cfs) outflows. The relative error between the two peak values was −1.0%.

Lastly, the observed time–of–rise was two hours later than the predicted one, corresponding to a −12.5% relative error. A cursory glance indicates that the two tracks are in approximate agreement. Outflow deviations, however, tend to be smoothed out with low rainfall totals. Fortunately flooding conditions rarely occur, if ever, with such small rainfall inputs.

March 28 was the next case study. The hydrograph shapes were in nearly complete agreement with one another. A two hour radar determined rainfall total of 0.90 inches was 0.06 inches lower than the observed rainfall excess value (0.96 in) before any infiltration rate reduction. Observed and predicted runoff volumes were only 10.7% apart.

In addition, the observed (3284 cfs) and predicted (3159 cfs) peak outflows showed only a small deviation. The times–of–rise for the observed and predicted tracks were in close agreement (14 h). This case study demonstrates the application of hydrograph methodology to accurately forecast runoff from moderate rainfall.

The next precipitation event occurred two days later on March 30. Again the observed and predicted hydrographs matched closely. This time, the predicted track slightly overestimated the observed one. Antecedent moisture conditions or prewetting may have played a factor in this reversal. The predicted runoff was 18.7% higher than the observed runoff.

Other characteristics were in better agreement. The observed peak (3284 cfs) was 3.8% higher than the predicted peak outflow (3159 cfs). Again the time–of–rise durations were in close agreement (14 h). Since this is the second smallest basin (87.4 mi^2) considered, these results suggest that hydrograph technique accuracy may improve with decreasing basin size.

The fourth case study happened the following day, March 31. This hour long 0.47 inch downpour produced similar observed and predicted runoff responses. However, reduced radar rainfall accumulations (0.42 in) fell slightly below observed (0.46 in) and predicted (0.45 in) rainfall excesses. Total runoff volumes varied by only 2.5%.

The observed peak (1792 cfs) was slightly higher than the predicted one (1660 cfs). The forecast time–of–rise (14 h) was one hour ahead of the observed period (15 h). All hydrograph variable results indicate strong agreement with each other.

The next precipitation event occurred on 15 May (see Fig. 10). The hydrograph shapes were similar although the predicted track considerably underestimates the volume and peak outflows. Again the radar derived accumulation was small (0.19 in). The observed rainfall excess (0.27 in) was 0.12 inches higher than the predicted total (0.15 in).

Likewise, a runoff volume disparity of 45.2% was measured. Peak outflow was underestimated by 35.5%. Even the times–of–rise produced a relative error of −17.6%. Results on low precipitation producing storms tend to vary considerably. The basin radar coverage indicated one hundred percent measurable precipitation reflectivities. Most of these reflectivities were small and may not have produced rainfall.

The sixth precipitation occurrence took place on June 27. The radar data ended before the second hump on the runoff hydrograph, track. Therefore, hydrograph analysis will only concentrate on the earlier times and a further comparison on the complete hydrograph would not be meaningful.

Again the predicted track appeared to underestimate the observed outflow. The predicted peak (1067 cfs) was 16.1% lower than the observed outflow (1272 cfs). Times–of–rise for both tracks are only one hour apart.

The last case study occurred on October 19. Very little correlation existed between the two tracks. The 0.11 inch radar determined accumulation clearly underestimated the observed outflow. The reduced accumulation (0.06 in) strongly deviates from the measured rainfall excess (0.21 in). Again the pattern of underestimating the observed track was related to low rainfall (<0.25 in).

The disparity between the observed and predicted runoff volume was 69.7%. The margin of error between the peak outflows was also large (40.9%). Even the times–of–rise varied up to 26.3%. The unit hydrograph response to small rainfall inputs does not produce substantial results.

3. *Loyalhanna Creek Hydrograph Analysis*

Loyalhanna Creek was the third test basin. It is the second largest (172 mi^2) and has the most forest coverage (71.0%). The comparisons are summarized in Table 4.

The first precipitation event occurred on March 20. The observed track closely paralleled the observed path, even to the point of describing a subtle kink on the rising limb. The predicted track slightly overestimated the volume and peak runoff quantities. The radar determined rainfall accumulation was measured over a twenty hour period. Radar rainfall estimates totalled 2.54 inches. The observed rainfall estimate excess was 1.20 inches, a significant difference from the radar determined value. But once each rainfall period was reduced by the 0.08 in / h infiltration rate, the excess rainfall values were only 6.7% apart.

In addition, the predicted and observed runoff volumes compared quite well with only a 6.2% difference separating the two quantities. The predicted peak runoff (5397 cfs) exceeded the observed quantity (4864 cfs). Both the observed and predicted times to the peak value were 25 hours. However radar bin coverage totalled only 36% indicating several isolated cells were the cause of runoff.

March 25 was the next precipitation producing day. The hydrograph shapes are similar in form. Variation near the downside of the observed crest was not identified on the predicted

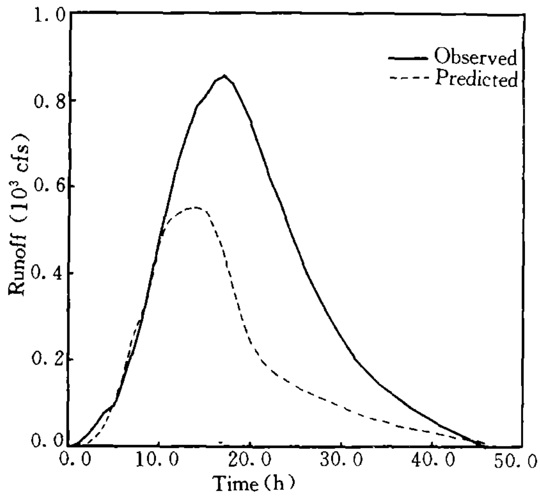

Fig. 10. Observed and predicted hydrograph tracks for Little Mahoning Creek, 15 May 1989.

track. The predicted runoff volume exceeded the observed value by 27.9%. As in the previous case, the rainfall total extended over a longer time. The 0.71 radar accumulation was assessed over a 5–h period. Reducing the hourly radar rainfall increments by the infiltration rate yielded a total rainfall amount of 0.31 inches. This value was somewhat higher than the observed rainfall excess (0.23 in).

Table 4. Rainfall Characteristics for Loyalhanna Creek

Date 1989	20 March	25 March	4 April	28 June	5 July
Radar rainfall (in)	2.54	0.71	0.86	1.34	1.16
Duration (h)	20	5	4	4	10
Basin radar coverage (%)	36	30	60	66	44
Observed runoff volume (mcf)	486.1	93.9	179.7	325.0	249.4
Predicted runoff volume (mcf)	516.1	120.3	161.4	393.2	168.0
Absolute error (mcf)	3.0	26.4	−18.3	68.2	−81.4
Relative error (%)	6.2	27.9	−9.8	21.0	−32.6
Observed rainfall excess (in)	1.20	0.23	0.45	0.81	0.62
Predicted rainfall excess (in)	1.28	0.30	0.40	0.98	0.42
Absolute error (in)	0.08	0.07	−0.05	0.17	−0.20
Relative error (%)	6.7	30.4	−11.1	21.0	−32.2
Observed peak (cfs)	3864	1402	2211	5343	2087
Predicted peak (cfs)	5397	1549	2158	5288	2086
Absolute error (cfs)	533	147	−52	−55	−1
Relative error (%)	11.0	10.5	−2.4	−1.0	−0.1
Observed time–of–rise (h)	25	9	13	11	11
Predicted time–of–rise (h)	25	12	12	11	14
Absolute error (h)	0	3	−1	0	3
Relative error (%)	0	33.3	−7.7	0	27.3

Further, predicted peak outflow (1549 cfs) surpassed the observed peak outflow (1402 cfs) by 10.5%. Times–of–rise varied by three hours corresponding to a 33.3% difference. Overall, forecast variables compared well.

The third case study occurred on 4 April. The predicted hydrograph almost traced the observed runoff path. However the predicted track underestimated the duration of the runoff by 14 hours. The radar totalled 0.86 inches over the 4–h period. The reduced radar rainfall depth (0.42 in) compared favorably with the observed rainfall excess (0.45 in). Predicted and observed runoff volumes differed by only 9.8%.

The difference between the observed (2211 cfs) and predicted (2158 cfs) peaks amounted to just 2.4%. A high correlation also existed between the times–of–rise. The relative error between the two durations was −7.7%. Rainfall quantities were the highest for Loyalhanna Creek, and hydrograph runoff tracks improved considerably with the increased rainfall amount.

June 28 was the next precipitation event. Another high rainfall occurrence, precipitation totalling 1.34 inches over a 4–h span. The predicted and observed hydrographs displayed strong resemblances, especially with respect to the rising limb and the baselength duration. The predicted track slightly overestimated the observed receding limb. As a result, the predicted volume exceeded the observed total by 21%.

Reduced radar determined rainfall (1.03 in) overestimated actual rainfall excess (0.81 in) by 0.22 inches. Peak output volumes were nearly the same. The observed maximum output (5343 mcf) surpassed the predicted total (5288 mcf) by 1%. In addition, the times to peak outflow were identical. Both tracks reached their respective peaks after 11 hours of runoff. Again runoff characteristics show close agreement with significant precipitation totals.

The last case study occurred on 5 July. A total of 1.16 inches of rain fell over a 9–h period. Radar bin coverage was only 44%. The predicted and observed hydrographs had similar shapes but the predicted track failed to duplicate the fine details in the measured flow. In addition, the predicted flow generally underestimated the observed outflow.

Runoff volume discrepancies reached 32.6%. The infiltration reduced radar estimated rainfall depth measured 0.44 inches, approximately 0.18 inches lower than the observed rainfall excess (0.62 in). However, maximum outflow forecasting was the best of all the case studies. The predicted peak (2086 cfs) reproduced the observed maximum outflow (2087 cfs) to within 1 cfs. The times to peak varied by over 27%.

4. *Mahoning Creek Hydrograph Analysis*

Mahoning Creek was the fourth basin to be examined. It is 158 mi^2 and has the flattest slop (9.51 ft / mi). The hydrograph analysis is summarized in Table 5.

Table 5. Rainfall Characteristics for Mahoning Creek

Date 1989	18 March	15 May	24 June	27 June	28 June
Radar rainfall (in)	0.22	0.27	1.27	0.29	0.11
Duration (h)	1	2	10	1	1
Basin radar coverage (%)	54	99	66	84	85
Observed runoff volume (mcf)	75.0	84.7	333.7	111.0	53.9
Predicted runoff volume (mcf)	63.0	61.6	315.5	87.3	22.3
Absolute error (mcf)	−12.0	−23.1	−18.2	−23.7	−31.6
Relative error (%)	−16.0	−27.3	−5.5	−21.4	−58.6
Observed rainfall excess (in)	0.20	0.23	0.91	0.30	0.15
Predicted rainfall excess (in)	0.17	0.16	0.86	0.24	0.06
Absolute error (in)	−0.03	−0.07	−0.05	−0.06	−0.09
Relative error (%)	−15.0	−30.4	−5.5	−20.0	−60.0
Observed peak (cfs)	992	988	3778	1493	435
Predicted peak (cfs)	793	783	3472	1120	280
Absolute error (cfs)	−199	−205	−306	−373	−155
Relative error (%)	−20.1	−20.7	−8.1	−25.0	−35.6
Observed time–of–rise (h)	17	16	21	15	32
Predicted time–of–rise (h)	16	17	20	16	16
Absolute error (h)	−1	1	−1	1	−16
Relative error (%)	−5.9	6.3	−4.8	6.7	−50.0

The first case study occurred on 18 March. A 1–h measured depth of 0.22 inches produced a predicted track that underestimated the majority of the observed hydrograph with the exception of the final portion of the receding limb.

The observed runoff volume exceeded the predicted sum by 16%. An infiltration rate of 0.05 in / h reduced the radar derived total to 0.17 inches. The observed rainfall excess (0.20 in) slightly surpassed this quantity. The predicted peak (793 cfs) also underestimated the observed peak (992 cfs) by 20.1%. The times of rise matched closely. The predicted peak (16 h) differed by one hour from the observed peak time (17 h).

The second case study on 15 May closely paralleled the first one in many respects. Again the predicted track underestimates the observed one. Like the previous case the radar derived rainfall (0.27 in) was small. In addition, a rainfall perturbation on the observed track was not illustrated in the forecast path.

The observed rainfall excess (0.23 in) exceeded the reduced radar determined total (0.17 in). Furthermore, the observed peak crested at 988 cfs nearly 21% higher than the predicted peak (783 cfs). The times–of–rise were similar. The predicted peak (17 h) occurred one hour after the observed time (16 h). The tendency to underestimate the observed hydrograph frequently exists with low rainfall amounts, resulting in wide variations in total runoff volume, rainfall excess, and peak outflow.

June 24 was the next case study. This time the rainfall was considerably greater (1.27 in). Accordingly, the hydrograph were similar, especially the two rising limbs. The predicted path slightly underestimated the crest and the duration of the time base. Runoff volumes corresponded well. The observed runoff volume exceeded the predicted one by 5.5%. The predicted peak (3472 cfs) lagged the observed peak (3778 cfs) by 8.1%. The observed time–of–rise (21 h) exceeded the predicted duration by one hour.

The fourth precipitation event took place on 27 June. Hydrograph shapes compared with each other, but the size of the observed track was larger. The radar derived rainfall (0.29 in) was small and when reduced by the infiltration rate (0.05 in / h), rainfall underestimated the observed rainfall excess (0.30 in). Likewise, the runoff volume is underestimated by 21.4%.

In addition, the observed runoff peak (1493 cfs) surpassed the predicted peak (1120 cfs) by 25%. Again, the times to rise match closely. For the fourth consecutive time, the duration difference was one hour, corresponding to a 6.7% relative error. The possibility of an adjustment or compensation for low rainfall generated depths should be explored.

The last case study occurred the next day on 28 June. The radar rainfall was very small (0.11 in). There was very little resemblance between the two plots. Pre–wetting conditions do not appear to play any role in the runoff hydrograph. Runoff volumes were underestimated by 58.6%.

The observed rainfall excess (0.15 in) surpassed the radar reduced depth (0.06 in) by 0.09 in. Peak runoff disparities were also outstanding. Peaks varied by 35.6%. However, the most striking difference occurred will be the times–of–rise. The observed rise peaked 16 hours after the predicted time–of–rise.

5. *Turtle Creek Hydrograph Analysis*

Turtle Creek was the last basin to be analyzed. It is the smallest watershed (55.9 mi^2). The analysis results can be found in Table 6.

Table 6. Rainfall Characteristics for Turtle Creek

Date 1989	18 March	31 March	18 April	17 June
Radar rainfall (in)	1.04	0.66	0.14	0.28
Duration (h)	2	1	1	3
Basin radar coverage (%)	82	95	96	100
Observed runoff volume (mcf)	217.1	209.7	80.1	40.4
Predicted runoff volume (mcf)	257.8	171.8	25.5	39.5
Absolute error (mcf)	40.8	−37.9	−54.6	−0.9
Relative error (%)	−18.8	−18.1	−68.2	−2.2
Observed rainfall excess (in)	0.77	0.75	0.28	0.14
Predicted rainfall excess (in)	0.92	0.61	0.09	0.14
Absolute error (in)	0.15	−0.14	−0.19	0
Relative error (%)	19.5	−18.7	−67.9	0
Observed peak (cfs)	6187	4367	1203	1249
Predicted peak (cfs)	5838	3810	562	867
Absolute error (cfs)	−349	−557	−641	−382
Relative error (%)	−5.6	−12.8	−53.3	−30.6
Observed time−of−rise (h)	7	8	6	9
Predicted time−of−rise (h)	7	7	7	8
Absolute error (h)	0	−1	1	−1
Relative error (%)	0	−12.5	16.7	−11.1

The first case study took place on 18 March. Approximately 1.04 inches covered the basin over a 2−h span. The shape of the predicted hydrograph matches the observed path with the exception of the overestimated recession limb. The predicted runoff volume exceeded the observed quantity by 18.8%.

An infiltration rate of 0.05 in / h reduced the radar rainfall depth to 0.94 inches. The observed rainfall excess measured 0.77 inches. The peak observed runoff (6187 cfs) for this event was more than for any basin studied. The predicted peak flow (5838 cfs) lagged the observed by 5.6%. The times−of−rise for this event both equaled seven hours. The time−of−rise showed a very fast response to the rainfall input. Flood potential would need to be carefully monitored.

The second precipitation event occurred on 31 March. Again, a large quantity of water (0.66 in) fell in a short period (one hour). Hydrographs compared favorably with one another. The predicted track slightly underestimated the observed path and was somewhat skewed to the left. In addition, the reduced radar determined rainfall (0.61 in) was 0.14 inches lower than the observed rainfall excess.

The observed runoff volume (209.7 mcf) exceeded the predicted volume (171.8 mcf) by 18.1%. The observed peak outflow (4367 cfs) also surpassed the predicted flow (3810 cfs) by 12.8%. The time−of−rise was one hour faster with predicted peak (7 h) than for the observed track (8 h).

The next runoff case study took place on 18 April. The predicted and observed hydrographs were in general agreement. The forecast track greatly underestimates the observed one. Also, several irregularities in the observed track are smoothed out in the predicted path.

Furthermore, the predicted runoff volume underestimates the observed volume by 68.2%. Only 0.14 inches of rain were measured by the radar. When reduced by the infiltration rate (0.05 in / h), the decreased or effective rainfall (0.09 in) vastly underestimates the observed rainfall excess (0.28 in). Peak outflow is another badly forecast characteristic. A −53.3% relative error marked the difference between the observed (1203 cfs) and predicted (562 cfs) peaks. The times of rise exhibited only a 1–h differential. This case exemplifies the forecast problems of low radar rainfall measurements.

The final precipitation input occurred on 17 June. Approximately 0.28 inches of rain were measured over a 3–h period. Again, as in the previous case, the fine details of the observed plot were damped out. The observed runoff rise at 6 hours probably was smoothed out by hourly radar reflectivity averaging. This problem appeared to be more common with low rainfall amounts. The predicted track also rose faster than the observed one. A more accurately depicted infiltration rate with a steep initial absorption curve would correct the discrepancy. However, the problem appears to be an isolated case.

In this instance, the reduced radar depth (0.14 in) equaled that of the observed rainfall excess (0.14 in). Likewise, the runoff volumes were similar. The relative error between the observed runoff volume (40.4 mcf) and the predicted one (39.5 mcf) accounted to −2.2%. The peak runoff, however, varied by 30.6%. Turtle Creek had another fast response time. The time–of–rise for the predicted track took eight hours, underestimating the observed period by one hour.

IV. DISCUSSION

Rainfall–runoff behavior can be analyzed by a variety of techniques including linear and nonlinear mathematical models. A simple and easy–to–apply linear approach is the unit hydrograph method. Basin runoff can be measured by combining unit hydrograph theory with radar derived precipitation accumulations. In extreme runoff scenarios, the method can be used to forecast flood conditions. Furthermore, hydrograph application is flexible and can be adapted to a wide variety of watersheds. This is illustrated for five basins in Pennsylvania.

Twenty–six rainfall events were examined in five basins. In 13 cases, the agreement was considered to be at least good, and sometimes excellent. In 12 cases, there were significant differences between the amplitude of the peak flow (and then usually also the runoff volume). A smaller problem seems to exist with time–of–rise or phase errors. Where only one or two events showed significant differences between the time of predicted and observed maximum runoff.

Successful runoff modeling can be traced to three distinct areas: unit hydrograph response curves, correct employment of hydrograph assumptions, and radar rainfall accounting. A failture in any one of the three categories will lead to erroneous results. Foremost, runoff prediction relies an accurate response curves. A large amount of discharge data are necessary to ensure a representative basin response function. Each watershed is assumed to have a unique runoff pattern. Consequently, predicted runoff is based on outflow following a similar pattern time after time.

Next, several assumptions must be adhered to obtain optimum results. The most important requires rainfall to have uniform spatial and temporal distribution. In addition, rainfall excess should range from 0.5 to 2.0 inches. A comparison of the eight most dissimilar hydrographs revealed an average radar derived rainfall of only 0.23 inches. In contrast, the mean radar basin coverage for these examples totalled 96.8%. The results suggest that hydrograph performance is more closely linked to quantity of rainfall excess than to basin's rainfall spatial distribution.

Finally, areal and temporal radar accumulations must reflect storm precipitation. Areal averaging and hourly averaging of six minute radar observations may not always be representative of the basin environment. Smaller basins and shorter convolution time steps may be necessary to improve runoff accuracy. In this experiment, observed runoff volumes consistently exceeded radar based accumulations, even without allowing for an infiltration rate.

Four criteria were used to evaluate the predicted runoff hydrograph with the observed one: overall shape, time–of–rise, peak outflow, and total runoff volume. The following list highlights the results from the five basins using the runoff algorithm.

- Hydrograph accuracy increased with increasing rainfall.
- Radar derived accumulations underestimated total rainfall especially during light precipitation. To compensate, infiltration rates used in this experiment were two to three times lower than those measured for similar soil type.
- The convolution procedure damped out irregularities in the observed runoff track. This problem was further magnified by areal and temporal radar reflectivity averaging.
- For all 26 cases, the time–of–rise was the easiest hydrograph characteristic to predict (87%).
- The forecast accuracies for the peak outflow and total runoff volume were 82.9% and 74.0% respectively.
- The basin (Turtle Creek) with the shortest unit hydrograph time of rise also had the shortest observed and predicted times of rise.
- For case studies with radar derived accumulations over 0.50 inches, the peak runoff became the most accurate forecast variable (94.5%).
- Forecast accuracy also improved for the other two variables within this rainfall category. The accuracy rate jumped to 90.7% and 83.5% for the time–of–rise and runoff volume.

Based upon these results, it is likely that greater success would be achieved if each basin was further divided into sub–basins and the rainfall, discredized in intervals of minutes, was used with the appropriated unit hydrograph to feed into the larger basin. This would most readily accommodate incomplete basin coverage (and spatial variability, the propagation of storms, and the temporal variability of storms).

REFERENCES

Bedient, P. B. and Huber, W. C. (1988), *Hydrology and Floodplain Analysis*, Addison–Wesley Publishing Comp., New York, pp.34—180.

Chezy, (1769), referred to in Rouse, H. and Ince, S. (1957), *History of Hydraulics*, Iowa Institute of Hydraulic Research, State University of Iowa.

Delleur, J. W. and Rao, A. R. (1973), Some extensions of linear systems analysis in hydrology, *Floods and Droughts: Proceedings of the Second Symposium in Hydrology*, Water Resources Publ., Fort Collins, 117pp.

Dragomar, J. H. (1990), A method to compare RADAP II radar rainfall to IFLOWS in real time, *NWS Eastern Tech. Attach.* No. 90–8B, pp.1—3.

Dunne, T. and Leopold, L. B. (1978), *Water in Environmental Planning*, W. H. Freeman and Comp., New York, pp.105—256.

Foster, E. E. (1948), *Rainfall and Runoff*, MacMillan Comp., New York, pp.293—314.

Gray, D. M. (1973), *Handbook on the Principles of Hydrology*, Water Information Council, Huntington, N.Y., Sect 7.

Horton, R. E. (1933), The role of infiltration in the hydrological cycle, *Trans Am. Geophys. Union*, **14:** 446—460.

Horton, R. E. (1935), Surface runoff phenomena, part I: analysis of the hydrograph, *Horton Hydrological Laboratory*, Voorhees, N.Y., pp.45—80.

Horton, R. E. (1945), Erosional development of streams and their drainage basins: hydrological approach to quantities morphology, *Bull. Geol. Soc. Amer.*, **56**: 275—370.

Leyton, L. Reynolds, E. R. C. and Thompsom, F. B. (1967), Rainfall interception in forest and moorland, *Forest Hydrology*, Pergamon Press, Oxford, pp.163—177.

Linsley, R. K., Koler, M. A. and Paulhus, J. L. H. (1949), *Applied Hydrology*, McGraw–Hill Book Comp., New York City, N.Y., pp.102—450.

Manning, R. (1889), On the Flow of water in Open Channels and Pipes, *Trans. Inst. Civil Engrs.*, Ireland, **20**: 161—207.

Marshall, J. S. and Palmer, W. M. (1948), The distribution of riandrops with size, *J. Meteor.*, **5**: 165—166.

Penman, H. L. (1948), Natural evaporation from open water, bare soil and grass, *Proceedings of the Royal Society of London*, Series A, **193**: 120—145.

Raudkivi, A. J. (1979), *Hydrology: An Advanced Introduction to Hydrological Processes and Modelling*, Pergamon Press, New York, 198pp.

Schaake, J. C. (1965), Synthesis of the Inlet Hydrograph, *Tech. Rept. No. 3, Dept. of Sanitary Eng. and Water Resources*, John Hopkins Unv., Baltimore pp.56—60.

Sheaffer, J. R. (1961), Flood–to–peak interval: Papers on Flood Problems, *Univ. of Chicago, Dept. of Geog. Res. Pap.*, **70**: 95—113.

Shaw, E. M. (1988), *Hydrology in Practice*, VNR International., London, pp.299—314.

Thornthwaite, C. W. (1948), An approach toward a rational classification of climate, *Geographic Review*, **38:** 55—94.

Viessman, W. Jr., Knapp, J. W., Lewise, G. L. and Harbaugh, T. E. (1977), *Introduction to Hydrology*, Harper and Row Publ., New York, pp.111—113.

Ward, R. C. (1967), *Principles of Hydrology*, McGraw–Hill Ltd., New York, pp.309—348.

Wetzel, K. L. and Bettandorff, J. M. (1986), Techniques for estimating streamflow characteristics in the eastern and interior coal provinces of the United States, U. S. Geol. Water–Supply Paper 2276.

Wilson, E. M. (1990), *Engineering Hydrology*, MacMillan Education Ltd., London, pp.23—170.